RSC Advances

ROYAL SOCIETY
OF CHEMISTRY

www.rsc.org/advances

Charge Density Distribution and Electrostatic Interactions of Ethionamide: An Inhibitor of enoyl acyl carrier protein reductase (inhA) enzyme of *Mycobacterium tuberculosis*

G. Rajalakshmi,[a] Mysore S. Pavan,[b] and P. Kumaradhas [*a,]

[a]Laboratory of Biocrystallography and Computational Molecular Biology
Department of Physics, Periyar University, Salem-636 011, India

[b]Solid State and Structural Chemistry Unit, Indian Institute of Science,
Bangalore 560 012, India

[*]Author to whom correspondence should be addressed: P. Kumaradhas
Corresponding author. Tel.: +91-(0)427-2345520, Fax: +91-(0)427-2345565.
E-mail address: kumaradhas@yahoo.com (P. Kumaradhas)

An experimental charge density analysis of an anti-TB drug ethionamide was carried out from high resolution X-ray diffraction at 100K to understand its charge density distribution and the electrostatic properties. The experimental results were validated from periodic theoretical charge density calculations performed using CRYSTAL09 at the B3LYP/6-31G** level of theory. The electron density $\rho_{bcp}(r)$ and the Laplacian of electron density $\nabla^2\rho_{bcp}(r)$ of the molecule calculated from both methods display the charge density distribution of ethionamide molecule in the crystal field. The electrostatic potential map shows a large electropositive region around the pyridine ring and a large electronegative region at the vicinity of thiol atom. The calculated experimental dipole moment is 10.6 D, which is higher than the value calculated from theory (8.2 D). The topological properties of C–H⋯S, N–H⋯N and N–H⋯S hydrogen bonds were calculated, reveals their strength. The charge density analysis of ethionamide molecule determined from both experiment and theory gives the topological and the electrostatic properties of the molecule, which allows precisely to understand the nature of intra and intermolecular interactions.

Abbreviations: *inhA*: 2 - trans enoyl acyl carrier protein reductase, *ethA*: Flavin monooxygenase, *NADH*: reduced form of Nicotinamide Adenine Dinucleotide, INH: isoniazid, ETH: ethionamide, MDR: multi-drug resistance.

Introduction

Tuberculosis remains the second leading infectious disease[1] causing high mortality in worldwide. Isoniazid, ethambutol, rifampicin and pyrazinamide are the first line drugs being used for the treatment at the initial stage of *Mycobacterium tuberculosis* disease.[2] These first line drugs are less effective for the treatment of *multidrug resistance tuberculosis* (MDR-TB).[3] Drugs such as thioamides, ethionamide (ETH), prothionamide are more effective against the MDR-TB; in which, ETH is the more efficacious, cheap and easily available drug and it is one of the second line drugs and the structural analogue of isoniazid (INH).[4,5] ETH is also a prodrug (Fig. 1) and it is should be activated by the enzyme to exert its antimicrobial activity,[6] the enzyme Flavinmonooxygenase (FMO) ethA[7] activates the ETH. EthA oxidizes the ETH moiety to form ETH-SO metabolite and 2-Ethyl-4-amidopyridine are exhibiting the biological activity like parent drug.[8] *In vitro* studies have identified other metabolites such as ETH-nitrite, ETH-aldehyde and ETH-OH.[9-11] The proposed active form of ETH is shown in Fig 1.

Like INH, ETH also targets the enoyl acyl carrier protein reductase (inhA) enzyme and inhibits the synthesis of mycolic acid.[12,13] The mutations in ethA gene, shows resistance to ETH; hence, it is essential to discover a new drug so as to target the inhA, without the activation by ethA enzyme.[14] Fig. 1 shows the molecular structure of ETH and its reactive species (Ethionamide S-oxide and 2-Ethyl-4-amidopyridine). In recent years, some derivatives of ETH drug molecules were synthesized and characterised in the quest to design anti-TB drugs with enhanced pharmacological activity. But to the best of our knowledge, yet there have been no quantitative structural analysis of such drugs, as it has utmost importance to understand the structure-activity relationship. The rational drug design requires precise knowledge about the drug-receptor interaction.
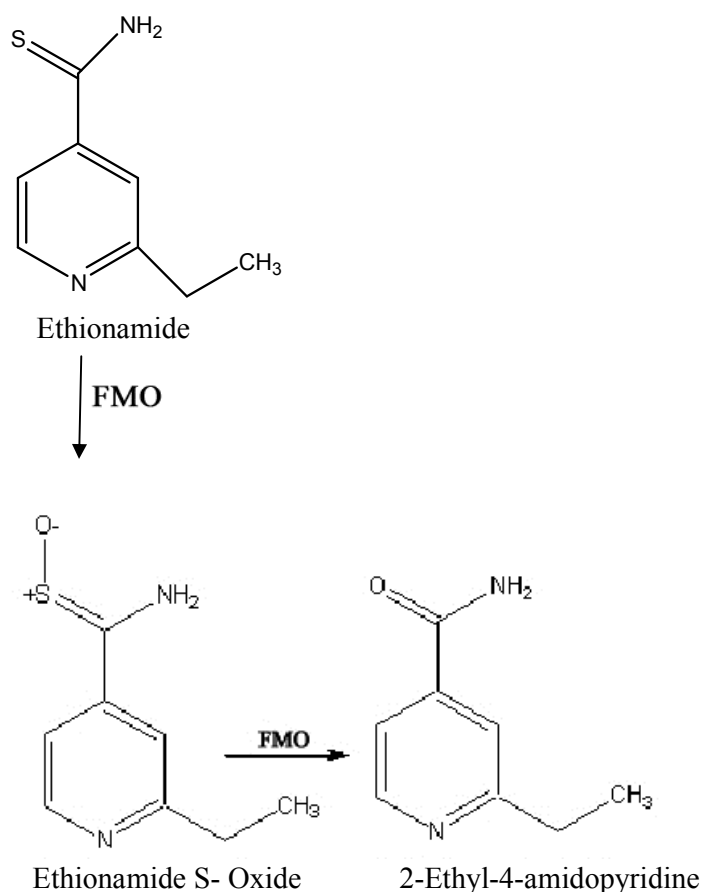
Fig. 1 Ethionamide and its reactive components: Ethionamide S-oxide and 2-ethyl-4-amidopyridine.[11]

The structure, conformation and charge density distribution of drug molecules play a very important role on binding of the same in the active site of receptor. Further, the biological recognition between drug and the receptor is achieved by intermolecular interactions and it mainly relies on the steric and complementary electronic properties.[15] Predicting such information from X-ray diffraction is immensely useful to derive potential lead compounds from the existing drug molecules. In this context, the conventional X-ray structure analysis provides the accurate molecular geometry and the geometry of hydrogen bonding interactions, π-stacking interactions and Van der Waals interactions, etc. But to obtain the accurate electronic structure, one has to rely on the technique of experimental charge density

3

analysis, which unravels the structure of molecules at electronic levels allowing to understand the charge density distribution and electrostatic properties of molecules in crystalline environment. The electrostatic properties (atomic charge, electrostatic potential and dipole moment) can be obtained from the experimental charge density analysis, which is an important property to predict the molecular recognition and reactivity, because, it depends on the electrostatic complementarity principle.[16] It is also widely used in biological sciences to understand the structural features.[17] In the present study, we have carried the charge density analysis of ETH from high resolution X-ray diffraction measured at 100K. The topological properties of electron density at the bond critical points (bcp) were determined; the electron density and the corresponding Laplacian of electron density at the bond critical point (bcp) give the charge density distribution of the molecule. The charge density distribution of the molecule is very sensitive to intermolecular interactions. The strength of each intermolecular interaction of ETH has been characterized using topological analysis of electron density. The electrostatic properties of the molecule have been determined, importantly, it displays the electrostatic surface of the molecule, which allows to identify the possible reactive locations of the ETH molecule; such locations of the molecule may interact with the complementary groups of the amino acids present in the active site of receptor to inhibit/kill the *Mycobacteria*. The experimental results have been compared with the periodic theoretical calculations of ETH molecule.

Experimental

The powder form of ETH compound was obtained from the Sigma-Aldrich Company. The ETH compound was crystallized from the saturated solution of ethanol solvent at room temperature using slow evaporation technique. Thus grown ETH crystals are found to be yellow in colour and exhibit good morphology with high transparency. From that, a high quality single crystal was chosen and mounted in Hampton Research Cryo-loops using

paratone-N oil for high resolution X-ray diffraction intensity measurements. The crystal was cooled by cold nitrogen gas stream to 100 K by using an Oxford Cryostream N_2 open-flow crysostat. The X-ray diffraction data was collected by using CrysAlisPro diffractometer[18] using MoKα radiation and the data reduction was also done by using CrysAlisPro software.[18] The high resolution data was collected upto the maximum resolution $(\sin\theta/\lambda)_{max}$=1.1 Å^{-1}. The total number of reflections measured was 54090; further, the reflections were sorted, merged and scaled by using SORTAV.[19] After merging, 8769 unique reflections (I≥2σ) were recovered to a resolution of $(\sin\theta/\lambda)_{max}$=1.1 Å^{-1}. The internal agreement factor for the final data set is R_{int}=0.0406 and R_{sigma}=0.024. The crystal structure was solved and refined by using spherical atom approximation F^2 method using SHELXS[20] and SHELXL[20] softwares respectively. Absorption correction was carried out by the numerical absorption correction based on Gaussian integration over a multifaceted crystal model as μ=0.336 mm^{-1}. The hydrogen bonding interactions were plotted using PLATON[21] software.

CCDC-1000256 contains the supplementary crystallographic data for this paper. These data can be obtained free of charge via www.ccdc.cam.ac.uk/conts/retrieving.html (or from the Cambridge Crystallographic Data Centre, 12 Union Road, Cambridge CB21Ez, Uk; fax: (+44)1223-336; or e-mail:deposit@ccdc.cam.ac.uk).

Multipole refinement

The electron density of ETH was modelled using Hansen-Coppens multipole formalism implemented in XD2006.[22] In the Hansen Coppens model,[23] electron density of each atom is represented as a sum of core electron density (ρ_{core}), a spherical valence electron density (ρ_{val}), and an aspherical part of the atomic electron density. R_l are appropriate radial functions

and Y_{lm} represents the spherical harmonics. The κ is the contraction-expansion parameter which modifies the radial distribution of the valence electron density and κ' are the expansion and contraction parameter of the radial part of aspherical valence shell. P_{lm} is the multipole population parameters.

$$\rho_{atom}(r) = P_c\rho_c(r) + P_v\kappa^3\rho_v(\kappa r) + \sum_{l=0}^{l_{max}}\kappa'^3 R_1(\kappa'r)\sum_{m=0}^{l}P_{lm\pm}Y_{lm\pm}(\theta, \phi)$$

Since the space group of ETH crystal is *I*a, it is non-centrosymmetric in nature; hence the origin was fixed[24] with reference to the co-ordinates of sulphur atom S(1). During the refinements, a single scale factor was refined for the whole resolution range of data. Subsequently, a high order refinement (sinθ/λ > 0.8 Å^{-1}) was performed to obtain the accurate positional and thermal parameters. During the high order refinement the X−H bond lengths were constrained to the neutron diffraction values.[25]

During the multipole refinements, sulphur atom was truncated at the hexadecapole level while for C and O atoms the refinement was done upto octupole level. κ and κ' for atoms with different chemical environments were assigned. For hydrogen atoms, the valence population and the bond directed dipole d_z was refined initially. Subsequently, the geometry obtained from high order refinement was used to obtain the anisotropic thermal displacement parameters of hydrogen atom by using SHADE2[26] approach. Thus obtained ADP's of hydrogen atoms were fixed and the bond directed quadrupoles (q_{3z^2}-1) of all hydrogen atoms were refined in the multipole modelling. For H atoms, the κ and κ' were fixed as 1.2. The geometrical parameters such as bond lengths, bond angles and torsion angles were calculated from XDGEOM routine of XD2006.[22] The topological properties of the electron density of ETH molecule were derived from the XDPROP routine of XD2006.[22] The Hirshfeld

rigid bond test[27] was performed for all covalent bonds, shows that the largest difference of mean-square displacement amplitude (DMSDA) is less than 5×10^{-4} $Å^2$, which is an indicator of the quality of data; and further from the value of DMSDA, it can be concluded that the atomic thermal motion of ETH has been well deconvuluted. The electrostatic potential (ESP) map has been plotted using XDGRAPH routine of XD2006,[22] The shown aminoacids are the pictorial representation which are forming interaction with ETH in the active site.

Theoretical calculations

A periodic theoretical calculation was performed for the ETH molecule using CRYSTAL09,[28,29] in this calculation the molecular geometry obtained from the experimental multipole refinement was used as an initial geometry. The quantum chemical calculation was carried out using the (DFT) B3LYP method[30] with the basis sets 6-31G**.[31] The shrinking factors (IS1-IS3) along the reciprocal lattice vectors were set at 4 (30 K points in the irreducible Brillouin zone). The truncation parameters were set as ITOL1 = ITOL2 = ITOL3 = ITOL4 = 6 and ITOL5=14. For better convergence the level shifter value was set to 0.6 Hartrees per cycle. The atomic position was fixed to the values obtained from the experiment. Multipole refinement for the theoretical structure factors was also carried out as the multipoles used in the experiment. Further, theoretical topological and electrostatic properties were calculated and compared with the experimental results.

Table 1 Experimental Details.

Chemical formula	$C_8N_2H_{10}S$
M_r	166.2
Cell setting, space group	Monoclinic, Ia
Temperature (K)	100(2)
a, b, c (Å)	7.1626(2), 14.9639(3), 7.9231(2)
$V(Å^3)$	801.01(3)
Z	4
D_x (g/cc)	1.378
Radiation type	Mo K_α
λ	0.71073
μ (mm^{-1})	0.336
Crystal form, color	Block, Yellow
Crystal size (mm)	0.21 x 0.43 x 0.82
Diffractometer	CrysAlisPro, Agilent, Technologies, Version 1.171.36.20
Data collection method	\ ω-scans
No. of observed reflections	8992
Criteria for observed reflections	$I > 2\sigma(I)$
F(000)	352
R_{int}	0.040
θ_{max} (°)	52.15
Range of h, k, l	$-15 \rightarrow h \rightarrow 15$
	$0 \rightarrow k \rightarrow 33$
	$-17 \rightarrow l \rightarrow 17$
Absorption correction	Gaussian (t_{min} = 0.7711, t_{max} = 0.9331)
Spherical atom model refinement	
$R(F), wR(F^2)$	0.025, 0.065
Absolute structure parameter	-0.003(16)
Goodness-of-fit	1.044
No. of reflections used in the refinement	8769
Multipole model refinement	
$R(F), wR(F^2)$	0.018, 0.042
Goodness-of-fit	1.185
N_{ref}/N_v	29.73
No. of reflections	8622
No. of parameters	290
$(\Delta/\sigma)_{max}$	0.0001
$\Delta\rho_{max}, \Delta\rho_{min}$ (eÅ^{-3})	0.20, -0.38

Results and discussion

Molecular structure and Intermolecular interactions. Fig. 2 displays the ORTEP[32] view of ETH molecule. The C–C bond lengths of ETH molecule contains pyridine ring ranges from 1.3939(4) to 1.4029(3) Å, the average value is 1.3993 Å. The bond lengths of C_{sp2}–C_{sp3} [C(1)–C(8): 1.4984(3) Å, C(4)–C(6): 1.5145(4) Å] bonds of the molecule are found to be unequal, the average value is 1.5062 Å; the C_{sp3}–C_{sp3} bond length C(6)−C(7) bond is 1.5281 Å. The S(1)–C(8) bond length is 1.6849(3) Å, which is almost agree with the reported bond length of room temperature structure.[33] The bond angle of the amide group H(2A)–N(2)–H(2B) is 118.4(3),° which is larger than the usual NH_2 bond angle, this difference is attributed to the involvement of the hydrogen atoms H(2A) and H(2B) in hydrogen bonding interactions. The torsion angle of C(5)–C(1)–C(8)–S(1) is -150.5(1)°, this wide angle bond twist indicates that, this bond exhibit *trans* conformation.
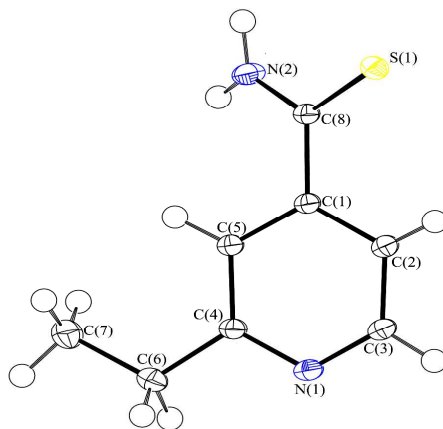
Fig. 2 An ORTEP view of ethionamide molecule, showing the atom numbering scheme. Displacement ellipsoids are drawn at 50% probability level and hydrogen atoms are shown as small spheres of arbitrary radii.

9

The dihedral angle between the pyridine ring and the plane of S(1), C(8) and N(2) atoms is 27.8,° indicates, these are not in co-planar. The complete details of geometrical parameters of the ETH molecule are presented in Table S1.

The crystal structure is stabilized by strong and weak hydrogen bonding interactions. Fig. 3, displays the hydrogen bonding interactions of ETH in the crystal. Each ETH molecule forms three hydrogen bonding interactions [C–H⋯S$^{(i)}$, and N–H⋯S$^{(ii)}$ and N–H⋯N$^{(iii)}$] with the symmetrically sitting neighbouring ETH molecules in the crystal; in which, the N–H⋯N$^{(iii)}$ interaction forms an infinite chain along the a-axis, while N–H⋯S$^{(ii)}$ forms an elongated chain approximately 123° from the N–H⋯N$^{(iii)}$ interaction (Fig. 3). The hydrogen bonding parameters of ETH molecule are presented in Table 2. [symmetry codes are: (i) -x,-y+1/2,z+1/2, (ii) x,y,z-1, (iii) x-1/2,-y,z]

Hirshfeld surface analysis[34] was carried out using Crystal Explorer3.0[35] to know the percentage contribution of intermolecular hydrogen bonding interactions of ETH. In ethionamide crystal C⋯H contacts contribute the highest percentage of about 50.3%, and the contributions of other intermolecular interactions are found to be in decreasing order; S⋯H (19.9%), N⋯H (19.3%), C⋯C (6.7%), C⋯N (1.6%) and N⋯N (0.3%). Thus, C⋯H contacts contribute the largest fraction for the stabilization of the ethionamide crystal structure.
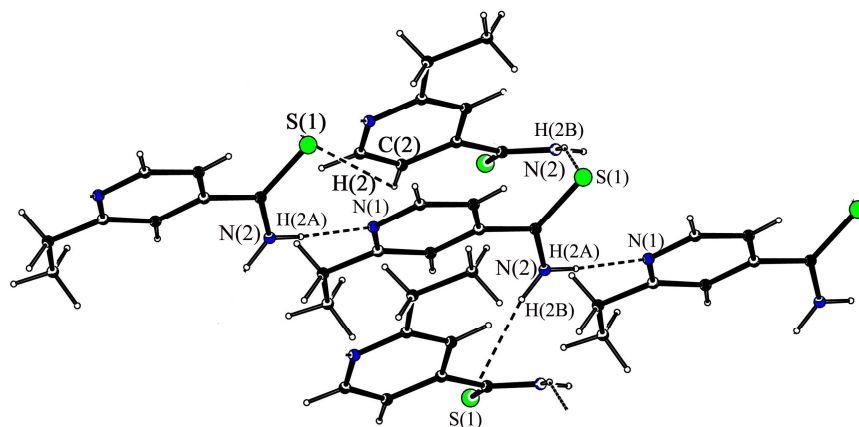
Fig. 3 Displaying the hydrogen bonding interactions.

Table 2 Intermolecular interactions (Å, º)

D–H⋯A	H⋯A	D⋯A	∠ D–H⋯A
C(2)–H(2)⋯S(1)[(i)]	2.966(15)	3.604	130.0(1)
N(2)–H(2A)⋯N(1)[(ii)]	2.064(15)	2.944	175.2(1)
N(2)–H(2B)⋯S(1)[(iii)]	2.637(15)	3.486	161.8(1)

(i) -x,-y+1/2,z+1/2, (ii) x,y,z-1, (iii) x-1/2,-y,z

Charge density distribution and Chemical bonding

The quality of the refined model was checked by the difference fourier map and the rigid-bond test.[27] The featureless residual density map (Fig. S1), shows the good agreement between the observed and calculated electron densities. The calculated topological properties of electron density allows qualitatively to characterize the covalent bonds, non-bonding interactions and the electronic structure of the molecule. The critical point (cp) search on all bonds in the molecule revealed a (3,-1) type of critical point named as bond critical point (bcp) for all bonds, which shows their covalent type character.[36] The molecular graph of ETH molecule (Fig. 4) displays the bond and ring critical points. The topological analysis

gives the electron density $\rho_{bcp}(r)$ and the Laplacian of electron density $\nabla^2\rho_{bcp}(r)$ at the bcp of each bond in the molecule, which are used to characterize the bond charge concentration or depletion.[37]
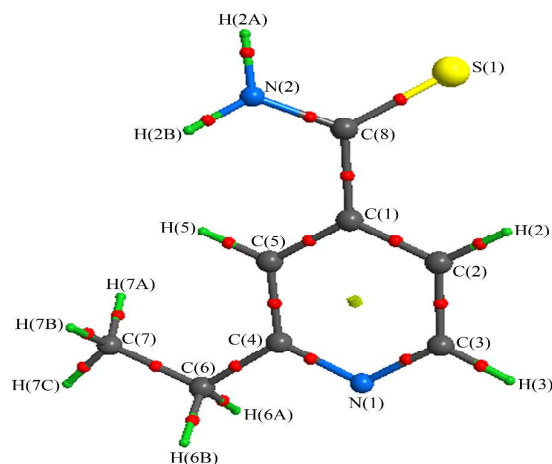
Fig. 4 The molecular graph of ethionamide molecule displays the (3,-1) and (3,+1) critical points. Big circle represents the atomic positions, small circle and square indicates the bond and ring critical points respectively.

The topological properties of electron density of ETH molecule is presented in Table 3. The electron density $\rho_{bcp}(r)$ of C–C bonds of ETH molecule contains pyridine ring ranges from 2.01(2) to 2.19(2) eÅ,$^{-3}$ indicates the moderate charge accumulation, the average value is 2.07 eÅ^{-3} ; this value is found to be higher than the other C–C [C(4)–C(6):1.69(2), C(6)–C(7): 1.64(2) and C(1)–C(8): 1.67(2) eÅ^{-3}] bonds of the molecule. Notably, the electron density $\rho_{bcp}(r)$ of S(1)–C(8) bond [1.49(5) eÅ^{-3}] is found to be less on compared with all other bonds in the molecule, this value is almost close to the reported values.[38,39] Surprisingly, the electron density of C–N [~2.28 eÅ^{-3}] bonds of ETH molecule contains pyridine ring and the C(8)–N(2) [2.29(3) eÅ^{-3}] bond are found to be almost equal. The electron density of C–H bonds of ETH molecule contains pyridine ring [~1.91 eÅ^{-3}] is

higher than the methyl [~1.81 eÅ^{-3}] and ethyl [~1.76 eÅ^{-3}] C–H bonds. The charge

accumulation in the amide N–H bonds (2.33 eÅ^{-3}) is relatively higher than all other bonds in

the molecule. The deformation density maps (Fig. 5) of ETH molecule displays the different

level of charge accumulation in various types of bonds and the position of lone pair electrons

of nitrogen atom in the molecule. The negative value of Laplacian of electron density

$\nabla^2\rho_{bcp}(r)$ at the bcp of all bonds indicates the presence of covalent type of interaction between

the atoms in molecule. The Laplacian of electron density of all C–C bonds of ETH molecule

contains pyridine ring are found to be highly negative on comparing with the other C–C

bonds present in the molecule; the average negative Laplacian of electron density of C–C

bonds is ~ -21.8 eÅ^{-5}, which confirms that the charges of these bonds are highly concentrated

than the other C−C bonds [C(4)–C(6): -13.3(1), C(6)–C(7): -12.2(1) and

C(1)–C(8): -13.9(1) eÅ^{-5}] bonds of the molecule; similar trend also observed the values

predicted by theory (Table 3). The $\nabla^2\rho_{bcp}(r)$ value of C–NH$_2$ bond is -31.3(1) eÅ^{-5}, which is

slightly higher than the C–N bonds [~ -29.4 eÅ^{-5}] of ETH molecule contains pyridine ring.

The $\nabla^2\rho_{bcp}(r)$ value of S(1)–C(8) bond[40] is -7.7(1) eÅ^{-5}; which is notably less negative,

indicates, the charges of the S–C bond is less concentrated on comparing with all other bonds

in the molecule and it is well match [-7.6 eÅ^{-5}] with the reported molecule[40] and further, this

value is also slightly less on compared with the calculated theoretical value (-8.1 eÅ^{-5})

(Table 3).

Table 3 Topological properties of electron density of ethionamide[a] [First line indicates experimental value, second line indicates the values obtained from the periodic calculation using the B3LYP/6-31G** method].

Bonds	$\rho_{bcp}(r)$ $e\text{Å}^{-3}$	$\nabla^2\rho_{bcp}(r)$ $e\text{Å}^{-5}$	λ_1 $e\text{Å}^{-5}$	λ_2 $e\text{Å}^{-5}$	λ_3 $e\text{Å}^{-5}$	ε	d_1 Å	d_2 Å	D Å	$\Delta d\%$
C(1)–C(2)	2.13(2)	-22.7(5)	-16.4	-12.9	6.6	0.260	0.729	0.671	1.400	2.07
	2.07	-17.3	-14.9	-12.7	10.3	0.17	0.721	0.679	1.400	1.50
C(1)–C(5)	2.01(2)	-19.8(1)	-14.9	-11.7	6.8	0.270	0.702	0.702	1.404	0.00
	2.06	-17.2	-14.9	-12.7	10.3	0.17	0.716	0.687	1.403	1.03
C(2)–C(3)	2.19(2)	-22.9(1)	-16.4	-13.5	7.0	0.210	0.680	0.715	1.394	1.26
	2.12	-18.7	-16.0	-13.1	10.4	0.22	0.683	0.711	1.394	1.00
C(4)–C(5)	2.07(2)	-21.0(5)	-15.6	-11.9	6.5	0.300	0.708	0.694	1.402	0.50
	2.11	-18.3	-15.8	-12.5	10.0	0.26	0.714	0.687	1.401	1.00
C(4)–C(6)	1.69(2)	-13.3(1)	-11.3	-10.0	7.6	0.180	0.812	0.705	1.517	3.53
	1.72	-11.6	-11.3	-10.8	10.5	0.05	0.797	0.718	1.515	2.61
C(6)–C(7)	1.64(2)	-12.2(1)	-10.4	-10.0	7.9	0.080	0.740	0.788	1.528	1.57
	1.58	-8.6	-9.8	-9.8	11.0	0.01	0.767	0.763	1.529	0.13
C(8)–C(1)	1.67(2)	-13.4(1)	-11.7	-10.0	8.2	0.170	0.710	0.788	1.499	2.60
	1.77	-12.3	-12.3	-11.2	11.2	0.09	0.747	0.752	1.499	0.17
C(3)–N(1)	2.29(3)	-28.4(1)	-17.9	-16.4	6.3	0.090	0.520	0.825	1.685	9.10
	2.30	-20.5	-18.5	-15.9	13.8	0.16	0.583	0.761	1.349	6.60
C(4)–N(1)	2.27(3)	-30.3(1)	-17.9	-15.8	3.3	0.130	0.829	0.520	1.349	11.45
	2.28	-20.3	-17.8	-15.2	12.7	0.18	0.771	0.578	1.349	7.15
C(8)–N(2)	2.29(3)	-31.3(1)	-19.7	-17.4	5.8	0.130	0.480	0.849	1.328	13.89
	2.34	-23.3	-18.2	-15.8	10.7	0.16	0.541	0.787	1.328	9.26
S(1)–C(8)	1.49(5)	-7.7(1)	-7.0	-6.30	5.6	0.100	0.822	0.863	1.685	1.22
	1.50	-8.1	-8.4	-6.5	6.7	0.29	0.822	0.864	1.686	1.25
C(2)–H(2)	1.90(7)	-22.0(3)	-17.6	-15.7	11.3	0.120	0.659	0.424	1.083	10.85
	1.87	-19.1	-17.3	-17.0	15.2	0.02	0.700	0.383	1.083	14.64
C(3)–H(3)	2.03(7)	-25.3(3)	-18.3	-17.4	10.4	0.050	0.645	0.438	1.083	9.56
	1.94	-20.0	-19.6	-17.7	17.3	0.11	0.717	0.366	1.083	16.21
C(5)–H(5)	1.79(7)	-17.8(2)	-16.0	-14.2	12.3	0.130	0.657	0.427	1.084	10.61
	1.91	-23.2	-20.2	-17.6	12.4	0.02	0.69	0.378	1.068	14.61
C(6)–H(6A)	1.80(8)	-20.3(2)	-15.8	-13.7	9.2	0.080	0.645	0.448	1.092	9.02
	1.87	-18.5	-16.7	-16.2	14.4	0.03	0.691	0.401	1.092	13.28
C(6)–H(6B)	1.72(8)	-15.4(3)	-13.6	-13.0	11.1	0.050	0.649	0.444	1.093	9.40
	1.82	-16.9	-16.2	-16.1	15.4	0.01	0.704	0.389	1.093	14.41
C(7)–H(7A)	1.90(9)	-17.8(4)	-15.8	-13.6	11.6	0.160	0.637	0.422	1.059	10.15
	1.91	-19.0	-18.1	-17.5	16.7	0.03	0.689	0.369	1.058	15.12
C(7)–H(7B)	1.83(8)	-19.8(2)	-14.9	-13.2	8.3	0.130	0.607	0.454	1.061	7.21
	1.93	-18.9	-18.2	-17.6	17.0	0.03	0.689	0.370	1.059	15.06
C(7)–H(7C)	1.71(8)	-14.3(2)	-12.4	-11.9	10.0	0.050	0.612	0.449	1.06	7.69
	1.99	-20.1	-18.7	-17.9	16.5	0.05	0.677	0.382	1.059	13.93
N(2)–H(2A)	2.30(9)	-28.4(5)	-28.5	-26.8	26.8	0.060	0.709	0.299	1.009	20.32

14

	2.28	-34.7	-31.8	-30.2	27.3	0.05	0.757	0.252	1.009	25.02
N(2)–H(2B)	2.35(9)	-27.1(4)	-28.3	-27.1	28.3	0.040	0.705	0.304	1.009	19.87
	2.29	-31.4	-35.0	-28.2	27.3	0.09	0.736	0.273	1.009	22.94

[a]$\rho_{bcp}(r)$ and $\nabla^2\rho_{bcp}(r)$, electron density and the Laplacian of electron density at the bcp; λ_1, λ_2, λ_3: eigen values; ε, bond ellipticity; d_1, d_2, the distance between bcp and each bonded atom; D, total bond path length; $\Delta d\%$, is the percentage of displacement of bcp from the midpoint of the bond.

(a)

(c)

(b)

(d)
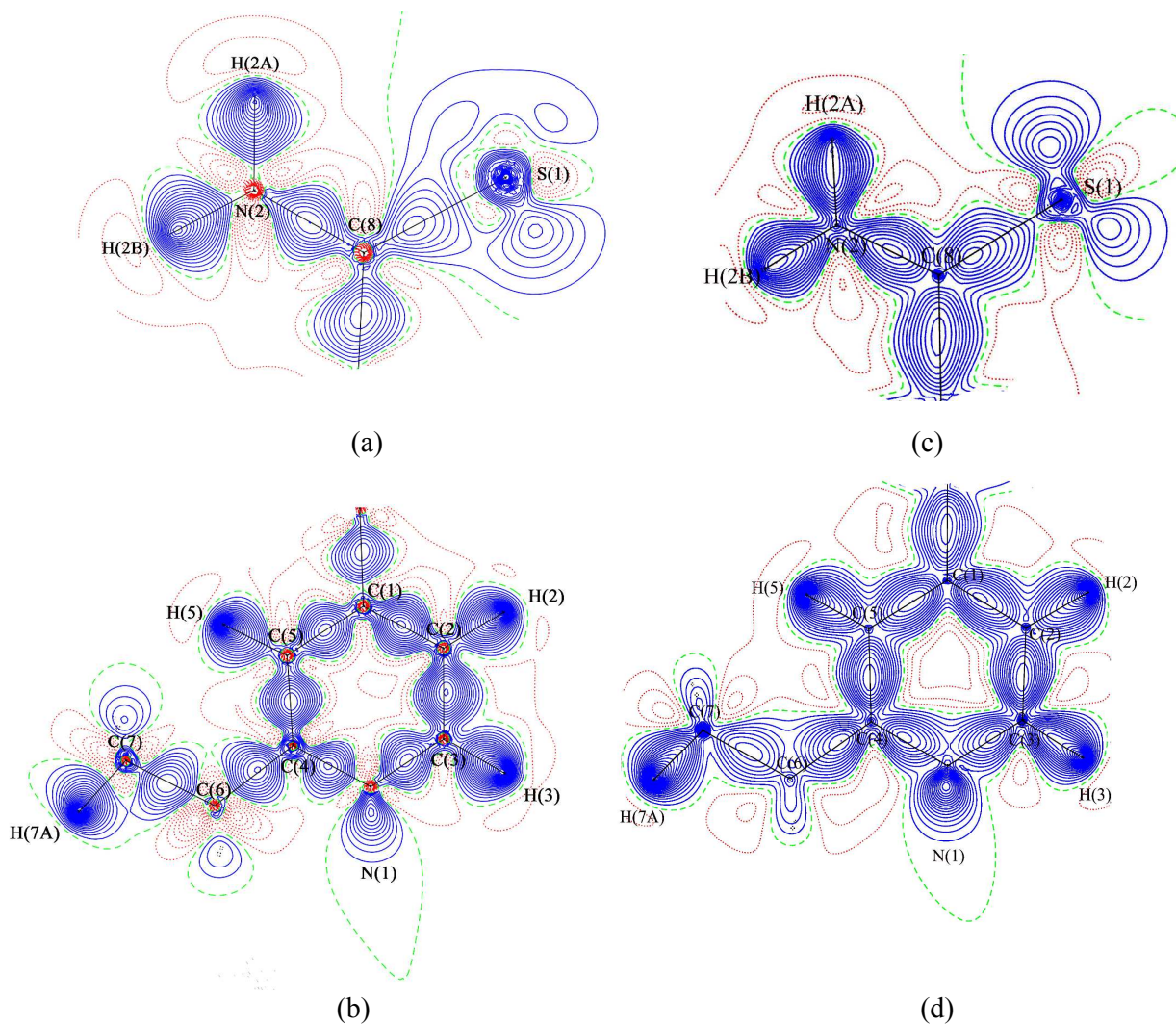
Fig. 5 The experimental (a,b) static and (c,d) the theoretical deformation density maps of ethionamide molecule. a) and c) are drawn at C(8), N(2), S(1) plane, b) and d) are drawn at C(1), C(3), C(4) plane. The contours maps are drawn at ±0.05 eÅ⁻³. Solid blue lines represent positive contours, red dotted lines are negative contours and the green dashed lines are zero contours.

The Laplacian of N–H bond is ~ -27.8 eÅ,$^{-5}$ the large negative value confirms that the charges of the bond is highly concentrated, this value is found to be lower than the theoretically observed values [~ -34.7 and ~ -31.4 eÅ^{-5}]. Overall, there is small discrepancy found between the theoretical and experimental electron density distribution. This difference can be well understood on careful investigation of the eigen values λ_1, λ_2 and λ_3 and also it may be due to the different behaviour of Gaussian and slater-type radial function at the

(a)   (b)
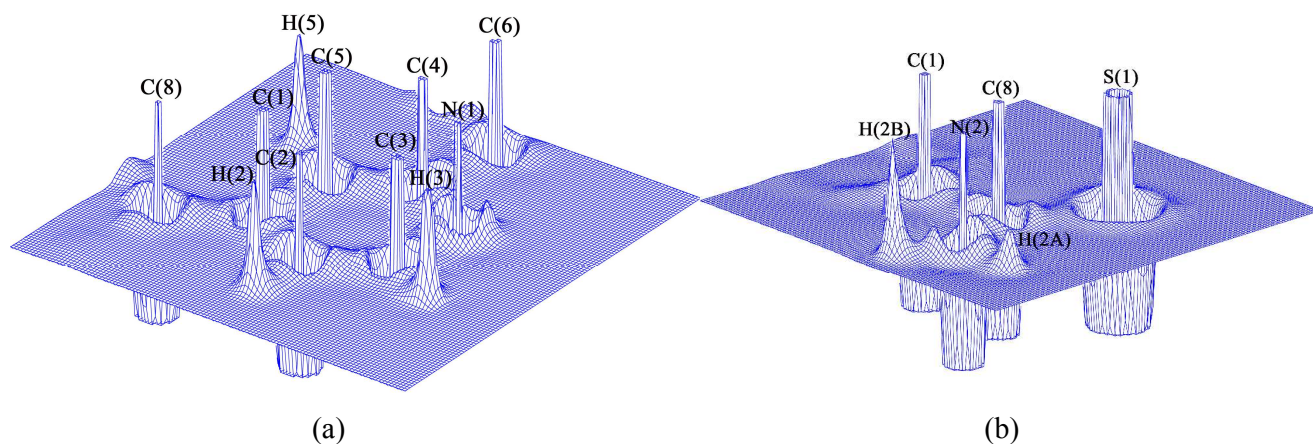
Fig. 6 The experimental relief maps showing the negative Laplacian of electron density of ethionamide molecule drawn in a) C(1), C(3), C(4) and b) C(8), N(2), S(1) planes. (range -250 to 250 eÅ^{-5}).

vicinity of bcp and the limited flexibility of basis set and electron correlation effects.[41,42] The values of $\rho_{bcp}(r)$ and $\nabla^2\rho_{bcp}(r)$ of S–C bond of ethionamide molecule from both experiment and theory are found to be small and this may be interpreted as a very weak shared interaction between the atoms.[40] The bonding nature of C and S atom in terms of charge density distributions of various molecules[38,40,43,44] are analyzed and found that the $\rho_{bcp}(r)$, $\nabla^2\rho_{bcp}(r)$ and R_{ij} of S–C bond of ethionamide molecule is almost similar to

1-formyl-3-thiosemicarbazide; thus, the S–C bond of ETH molecule shows partial double bond character.[38] This observation indicates the possible resonance character of the S–C bond. Overall, the charge concentration of C–N bonds is predominantly higher than all other bonds in the molecule, similar trend is also observed in theory. Fig. 6 represents the experimental relief map of ETH molecule. In relief map, the atom positions are represented by sharp peaks and the lone pair positions of nitrogen are also clearly visible. The curved surface between the atoms indicates the existence of bonds among the atoms present in the molecule.[45]

Bond ellipticity ε of all bonds in the molecule has been calculated (Table 3), which is a measure of charge accumulation in a plane perpendicular to the bond; it also allows to quantify the π-character and the extent of conjugation in a given molecule.[46] The experimental ellipticity values of all the bonds were found to be higher than the values predicted by DFT calculations. Notably, the ellipticity of C–C bonds of ETH molecule contains pyridine ring is ~ 0.2, which is relatively high, when compared with the other bonds in the molecule. This may be attributed to the large anisotropy of electron density and the π-bond nature. The small bond ellipticity values of S–C and C–N bonds, confirming their cylindrical nature.

Net atomic charges and Dipole moment

The experimental AIM charges of atoms and the corresponding atomic volumes of ETH were calculated using TOPXD[22] and the theoretical charges were calculated using QTAIM[37] program (Table 4). Among all atoms, the C(3) and C(8) atoms exhibit high positive charge (0.62e and 0.46e), while the S(1) and N(1) atoms are carrying high negative charge, the corresponding values are -0.84e and -0.98e respectively. The methyl hydrogen atoms H(7A) and H(7C) are slightly positive and this trend is also found in the reported paper.[46] The N(2)

atom is also negatively charged, the value is -0.97e, this high negative charge tends to have high positive charge in its attached hydrogen atoms H(2A) [0.40e] and H(2B) [0.32e]. The other hydrogen atoms carry less negative charge, and considered as electrically neutral. The atomic volume of carbon atoms ranges from 8.4 to 11.2 Å^3. The sulphur atom is larger in size, its volume is 33.8 Å^3. The volume of hydrogen atoms are ranges from 2.6 to 8.4 Å^3; these values are almost match with the reported molecule.[46] The total volume of all atoms in the unit cell is 801.0 Å^3, this volume is close to the experimental volume (Table 1) of unit cell (812.4 Å^3) with the difference of 11.4 Å^3; further, the periodic theoretical calculations also predicts relatively similar volume to the total volume of all the atoms present in the unit cell, the corresponding value is 800.8 Å^3. The experimental volume of H(2A), H(2B), N(1) and S(1) atoms are 2.6, 3.5, 14.6 and 33.8 Å^3 respectively, their corresponding theoretical volumes are 2.6, 3.2, 13.9 and 32.8 Å^3 respectively.

Gradient vector field

Fig. 7 shows the gradient vector field of ETH molecule plotted in two different planes C(1), C(3), C(4) and C(1), C(8) and N(1) using Winxpro software.[47,48] The electron density $\rho_{bcp}(r)$ of a molecule is a scalar quantity; it can also be expressed as a gradient vector field. The gradient trajectory originates at the minimum or the saddle point and terminates at the maximum point (atom) i.e., (basin). The basin is surrounded by a zero-flux surface and it is the boundary of the atom, shown in thick blue lines. The carbon atom looks like a prismatic form whereas sulphur atom looks like a drop shape. The calculated bond path analysis reveals the polarization of bonds in the molecule. The bcp lies at the middle of the homo atomic bonds can be viewed in both Fig. (6 & 7). The polarisation in hetero-atomic bonds such as the C−N bonds can be observed from the position of bcp's which are move towards the carbon atom, while in C−H and N−H bonds the bcp positions are shifted towards the electropositive

hydrogen atom. Among the non-hydrogen covalent bonds, C(8)–N(2) bond exhibits maximum polarization, where the degree of polarization is 13.9%. Further, the N–H bonds are found to be highly polar when compared with the C–H bonds. The average degree of polarization of N–H bond is ~20.1%.

Table 4 Atomic charges (e) and volumes ($Å^3$) of ethionamide molecule.

Atoms	Atomic charges		Volume	
	Experiment	CRYSTAL09	Experiment	CRYSTAL09
C(1)	0.10	0.02	9.9	9.6
C(2)	0.17	-0.03	11.2	11.4
C(3)	0.62	0.29	9.5	10.2
C(4)	0.20	0.33	9.1	8.1
C(5)	0.21	-0.04	9.6	10.1
C(6)	0.31	-0.04	8.4	8.6
C(7)	0.10	-0.15	10.3	10.8
C(8)	0.46	0.25	9.3	9.4
N(1)	-0.98	-0.88	14.6	13.9
N(2)	-0.97	-0.98	16.6	16.2
S(1)	-0.84	-0.29	33.8	32.8
H(2)	-0.02	0.12	6.7	6.4
H(2A)	0.40	0.47	2.6	2.6
H(2B)	0.32	0.43	3.5	3.2
H(3)	-0.04	0.09	6.6	6.3
H(5)	-0.06	0.07	6.2	5.8
H(6A)	0.06	0.06	6.4	7.0
H(6B)	-0.02	0.05	6.5	7.3
H(7A)	-0.12	0.10	7.1	6.6
H(7B)	-0.06	0.08	6.8	6.4
H(7C)	-0.16	0.03	8.4	7.5
			203.1	200.2
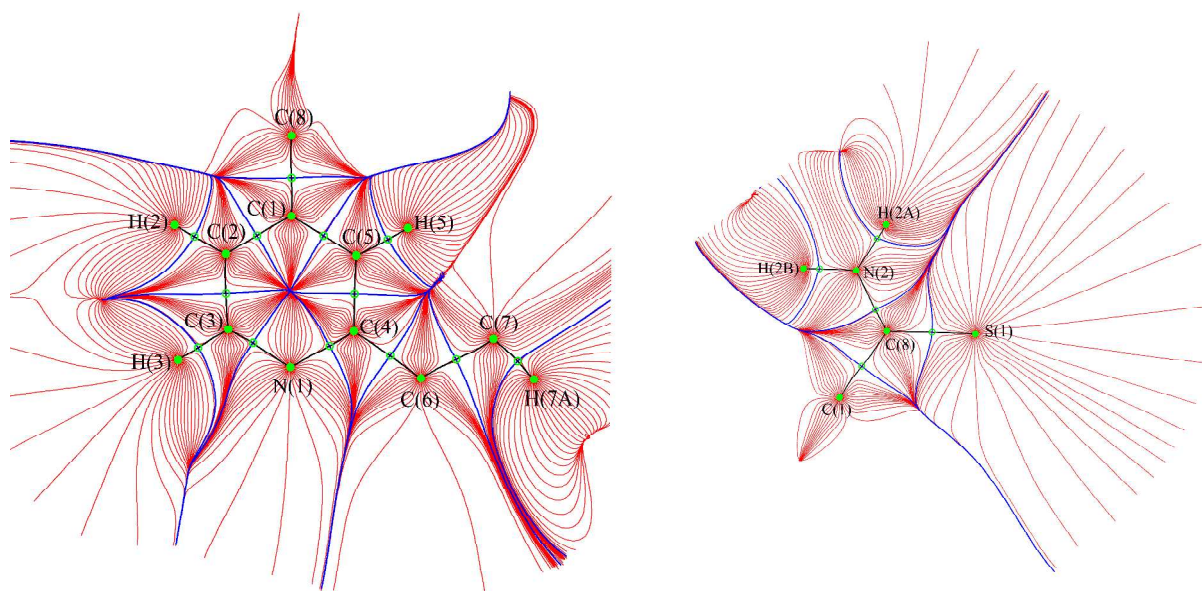
Fig. 7 Gradient trajectory plots of experimental electron density distribution of ethionamide molecule drawn in different planes C(1), C(3), C(4) and C(8), S(1), N(2). The closed blue thick solid lines around an atom are the boundaries of the atomic basin and the green open circles represent the (3,-1) critical points.

Electrostatic potential

Electrostatic potential (ESP) of the molecule is one of the derived electrostatic properties of molecules, which is directly related to the reactivity of the molecules.[49] It determines the reactive locations (nucleophilic and electrophilic sites) of the molecule and it is also used to predict the alignment of a drug molecule in the active site of its receptor.[50] Thus, it gives a clear pictorial view of drug-receptor interaction. In the present study, the ESP surface of ETH molecule has been obtained from the experimental multipole modelling; Fig. 8 displays the ESP surface of ETH molecule and interaction (pictorial view) with the neighbouring amino acids present in the active site; in which, the large electropositive surface over the ETH molecule contains pyridine ring forms an aromatic π-stacking interaction with the Phe149. The positive surface over the ethyl group of ETH also forms such π-stacking interaction with the Tyr158. The C(6) atom of the molecule exhibiting high positive charge, which is

20

covalently attached with the NADH to form ETH-NAD adduct. A large electronegative

region is found at the vicinity of thiocarbonyl atom. The experimental dipole moment of the

molecule is 10.6 D, which is higher than the value predicted by theory [8.2 D].
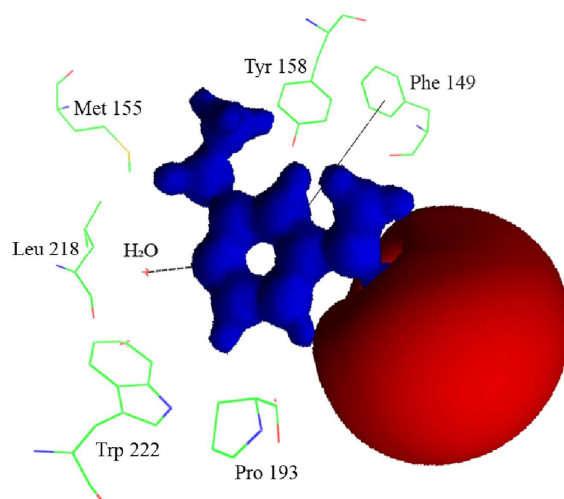
Fig. 8 The isosurface representation of molecular electrostatic potential map of ethionamide
molecule displays the possible ethionamide-receptor interactions. Positive potential drawn at
+0.5 eÅ^{-1} (blue) and the negative potential drawn at -0.05 eÅ^{-1} (red).

Topological properties of electron density of hydrogen bonding interactions

The topological analysis of electron density of three hydrogen bonds of ETH molecule

(Table 2) was carried out, reveals a (3,-1) type critical point for all listed hydrogen bonds.

The topological properties of hydrogen bonding interactions, local kinetic energy density,

potential energy density and local total energy density[51-53] are calculated (Table 5).   The

calculated energy density and bond dissociation energy (BDE) of the hydrogen bonding

interactions at the bcp gives the strength of the bond.[54] The bcp of C–H$\cdots$S$^{(i)}$ and

N–H$\cdots$S$^{(iii)}$ hydrogen bonds exhibit very less amount of electron density, the values are

0.06(1), 0.07(2) eÅ^{-3} respectively, and the corresponding Laplacian $\nabla^2\rho_{bcp}(r)$ values are found

to be positive [0.650(3), 1.15(2) eÅ^{-5}]. The electron density $\rho_{bcp}(r)$ and the $\nabla^2\rho_{bcp}(r)$ values of N(2)–H(2A)$\cdots$N(1)$^{(ii)}$ interaction is 0.18, 0.189 eÅ^{-5}, respectively; these values are slightly higher than H$\cdots$S$^{(i)}$ and H$\cdots$S$^{(iii)}$ interactions.[55,56] Further, the energetic parameters of C–H$\cdots$S$^{(i)}$, N–H$\cdots$S$^{(iii)}$ are of the order of $|V|/G < 1$ and $H(r) > 0$; from this, it is confirmed that these interactions are *closed shell* interactions;[57] whereas, the energetic parameters for N–H$\cdots$N$^{(ii)}$ are of the order of $|V|/G < 1$ and $H(r) < 0$, which indicates the existence of *partial covalent type* of interaction. The BDE of all hydrogen bonding interactions were calculated (Table 5), in which, N–H$\cdots$N$^{(ii)}$ interaction is notably stronger than C–H$\cdots$S$^{(i)}$ and N–H$\cdots$S$^{(iii)}$ interactions. Fig. 9 shows the Laplacian of electron density of N(2)–H(2A)$\cdots$N(1)$^{(ii)}$ and N(2)–H(2B)$\cdots$S(1),$^{(iii)}$ hydrogen bonding interactions in the crystal. [Symmetry code: (i) -x,-y+1/2,z+1/2, (ii) x,y,z-1, (iii) x-1/2,-y,z].

Table 5 Topological properties of hydrogen bonds[a]

Interactions	$\rho_{bcp}(r)$ eÅ^{-3}	$\nabla^2\rho_{bcp}(r)$ eÅ^{-5}	λ_1 eÅ^{-5}	λ_2 eÅ^{-5}	λ_3 eÅ^{-5}	d_1 Å	d_2 Å	R_{ii} Å	$G(r)$ a.u	$V(r)$ a.u	$H(r)$ a.u	D kcal/mol
C(2)–H(2)$\cdots$S(1)$^{(i)}$	0.06(1)	0.650(3)	-0.18	-0.13	0.96	1.0416	1.8100	2.8516	0.005	-0.004	0.0006	1.26
N(2)–H(2A)$\cdots$N(1)$^{(ii)}$	0.18(5)	1.89(10)	-1.20	-1.16	4.25	1.2928	0.6461	1.9389	0.02	-0.02	-0.0004	6.27
N(2)–H(2B)$\cdots$S(1)$^{(iii)}$	0.07(2)	1.15(2)	-0.26	-0.23	1.65	1,7242	0.7949	2.5192	0.009	-0.006	0.003	1.8

[a]G(r), V(r), H(r) represents the kinetic energy density, potential energy density, total energy density respectively;
D is the bond dissociation energy.
(i) x,-y+1/2, z+1/2, (ii) x, y, z-1, (iii) x-1/2,– y,z

(a)   (b)

(c)
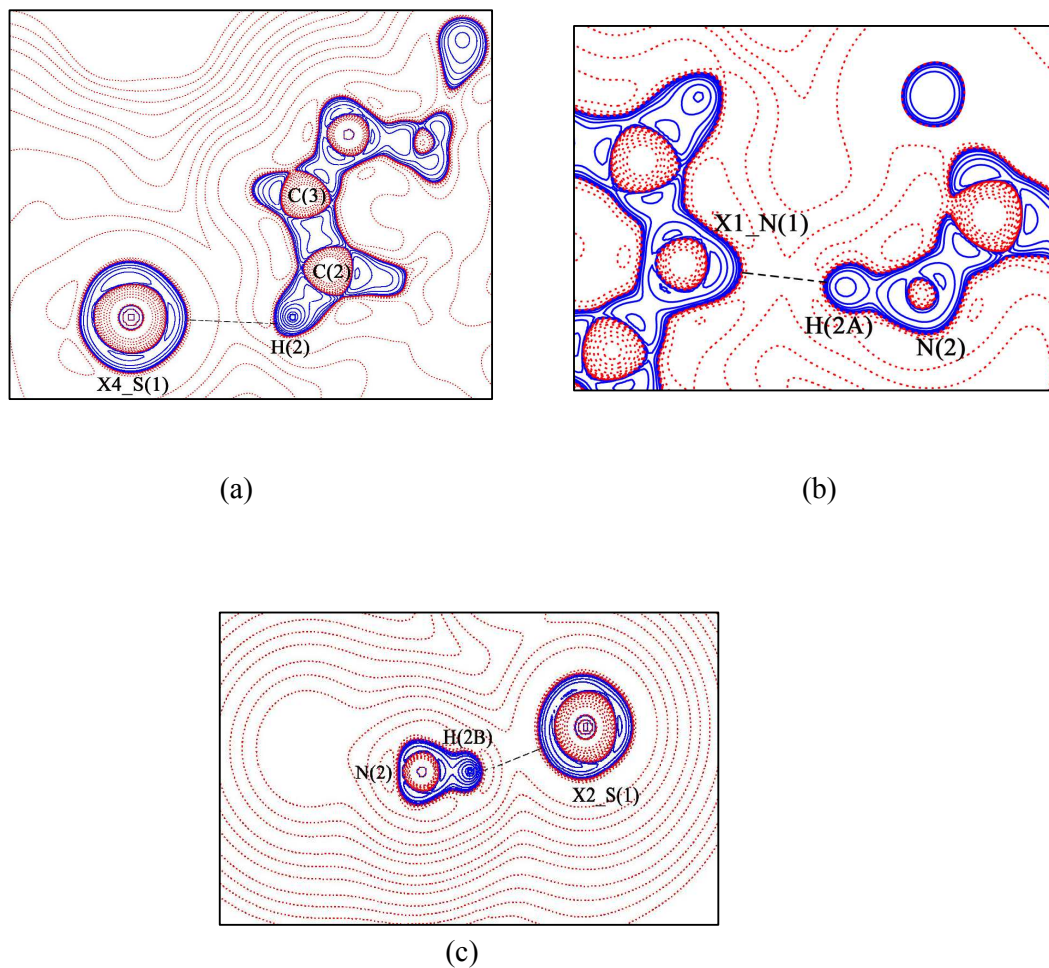
Fig. 9. Laplacian of electron density of a) C(2)−H(2)···S(1),[(i)] b) N(2)−H(2A)···N(1)[(ii)] and N(2)−H(2B)···S(1)[(iii)] hydrogen bonding interactions. Contours are drawn in logarithmic scale, 3.0×2^N eÅ^{-5}, where $N=2,4,8\times10^n$, $n= -2,-1,0,1,2$. Solid blue lines and dotted red lines represent positive and negative contours respectively.

Conclusions

The topological properties of electron density and electrostatic properties of ethionamide molecule were determined from the experiment and compared with the periodic theoretical calculations. The charge density distribution of ETH molecule determined from both experiment and theory reflects the topological properties of electron density at the bcp of all bonds in the molecule. Notably, the $\rho_{bcp}(r)$ and $\nabla^2\rho_{bcp}(r)$ of S–C bond is significantly less on compared with all other bonds in the molecule; this interprets the existence of very weak shared interaction between the atoms and the $\rho_{bcp}(r)$, $\nabla^2\rho_{bcp}(r)$ and R_{ij} value of S–C bond of ethionamide and its resonance nature. On the other hand, the electron density at the bcp of C–N bonds is found to be high and the charges are also highly concentrated. The S(1) atom is having larger atomic volume than all other atoms in the molecule. The experimentally determined unit cell volume is very much similar to the theoretically calculated atomic volume. The N(2)–H(2A)···N(1) interaction is *partially covalent type* character, while C–H···S and N–H···S exhibit *closed – shell* type of interactions. The charge density analysis of ethionamide molecule determined from both experiment and theory gives the topological and the electrostatic properties of the molecule, which allows precisely to understand the nature of intra and intermolecular interactions.

References

[1]   M. Flipo, M. Desroses, N. Lecat-Guillet, B. Dirie, X. Carette, F. Leroux, C. Piveteau, F. Demirkaya, Z. Lens, P. Rucktooa, V. Villeret, T. Christophe, H. Kyoung Jeon, C. Locht, P. Brodin, B. Deprez, A. R. Baulard and N. Willand, *J. Med. Chem.,* 2011, **54**, 2994–3010.

[2]   E. D. Chan and M. D. Iseman, *BMJ*, 2002, **325***, 1282–1286.

[3]   A. Mahmoudi and M. D. Iseman, *JAMA*, 1993, **270**, 65–68.

[4]   J. Crofton, P. Chaulet, D. Maher, J. Grosset, W. Harris, N. Horne, M. Iseman, B. Watt, Guidelines for the management of multidrug resistant Tuberculosis. World Health Organization, Geneva, Switzerland. 1, (1997).

[5]   J. S. Blanchard, *Annu. Rev. Biochem.*, 1996, **65**, 215–239.

[6]   A. E. DeBarber, K. Mdiuli, M. Bosman, L. G. Bekker, C. E. Barry and 3rd *Nat. Aca. Sci. USA.*, 2000, **97**, 9677–9682.

[7]   T. A. Vanneli, A. Dykman and P. R. O. Montellano, *J. Biol. Chem.*, 2002, **277**, 12824–12829.

[8]   J. P. Johnson, P. O. Kane and M. R. Kibby, *J. Pharm. Pharmacol.,* 1967, **19**, 1.

[9]   X. Hanoulle, J. M. Wieruszeski, P. Rousselot-Pailley, I. Landrieu, C. Locht, G. Lippens and A. R. Baulard, *J. Antimicrob. Chemother.*, 2006, **58**, 768–772.

[10]   P. J. Jenner, G. A. Ellard, P. J. K. Gruer and V. R. Aber, *J. Antimicrob. Chemother*. 1984, **13**, 267–277.

[11]   X. Hanoulle, J. M. Wieruszeski, P. Rousselot-Pailley, I. Landrieu, C. Locht, A. R. Baulard and G. Lippens, *Biochem. Biophys Res. Commun*. 2005, **331**, 452–458.

[12]   X. Hanoulle, J. M. Wieruszeski, P. Rousselot-Pailley, I. Landrieu, C. Locht, A. R. Baulard and G. Lippens, *Biochem. Biophys Res. Commun*. 2005, **331**, 452–458.

[13]   A. Quemard, G. Laneelle and C. Lacave, *Antimicrob. Agents. Chemother*. 1992, **36**, 1316–1321.

[14]   F. Wang, R. Langley, G. Gulten, L. G. Dover, G. S. Besra, W. R. Jacobs Jr., and J. C. Sachhettini, *J. Expt. Med.,* 2007, **204**, 73–78.

[15]   S. Mebs, A. Luth and P. Luger, *Bioorg. & Med. Chem.*, 2010, **18**, 5965–5974.

[16]   S. Grabowsky, T. Pfeuffer, W. Morgenroth, C. Paulmann, T. Schrimeister and P. Luger, *Org. Biomol. Chem.*, 2008, **6**, 2295–2307.

[17]   M. Mladenovic, M. Arnone, R. F. Fink and B. Engels, *J. Phys. Chem.,* 2009, **B113**, 5072–5082.

[18]   CrysAlisPro, Agilent Technologies, Version 1.171.36.20 (release 27-06-2012 CrysAlis171. NET).

[19]   R. H. Blessing, *J. Appl. Crystallogr.,* 1997, **30**, 421–426.

[20]   G. M. Sheldrick, SHELXS-97, and SHELXL-97, Programs for Crystal Structure Analysis & refinement (Release 97-2), Institut fur Anorganische Chemie der Universitat: D-3400 Gottingen, Germany, 1998.

[21]   A. L. Spek, PLATON, A Multipurpose Crystallographic Tool, Utrecht University, Utrecht, The Netherlands, 1998.

[22]   T. Koritsanszky, P. Macchi, C. Gatti, L. J. Farrugia, P. R. Mallinson,
         A. Volkov and T. Richter, *XD-2006.* A Computer Program Package for
         Multipole Refinement and Topological Analysis of Charge Densities and
         Evaluation of Intermolecular Energies from Experimental or Theoretical
         Structure Facto*rs*, Version 5.33, 2007.

[23]   N. K. Hansen and P. Coppens, *Acta Crystallogr. Sect. A: Found. Crystallogr.,*
         1978, **34**, 909−921.

[24]   Deepak Chopra, T. N. Guru Row, E. Arunan and Roger A. Klein. *J. Mol.
         Struct.,* 2010, **964**, 126-133.

[25]   F. H. Allen, O. Kennard, D. G. Watson, L. Brammer, O. Guy and R. Taylor,
         Tables of Bond length determined by X-Ray and Neutron Diffraction. Part 1
         Bond lengths in organic compounds, *J. Chem. Soc. Perkin Trans.,* 1987, **2**,
         S1−S83.

[26]   A. O. Madsen, *J. Appl. Crystallogr.,* 2006*,* **39**, 757−758.

[27]   F. L. Hirshfeld, *Acta Crystallogr. Sect. A: Found. Crystallogr.,* 1976, **A32**,
         239−244.

[28]   R. Dovesi, R. Orlando, B. Civalleri, C. Roetti, V. R. Saunders and C. M.
         Zicovich-Wilson. *Z. Kristallogr*., 2005, **220**, 571−573.

[29]   R. Dovesi, V. R. Saunders, C. Roetti, R. Orlando, B. Civalleri, C. M.
         Zicovich-Wilson, F. Pascale, B. Civalleri, K. Doll, N. M. Harrison, I. J. Bush,
         P. D' Arco and M. Llunell. 2009, CRYSTAL09 User's Manual. University of
         Torino, Italy.

[30]   R. G. Parr and W. Yang. *Density Functional Theory of Atoms and Molecule,*
         Oxford University Press: London, 1989.

[31]   P. C. Hariharan and J. A. Pople. *Theor. Chim. Acta*, 1973, **28,** 213−222**.**

[32]   L. J. Farrugia. *J. Appl. Cryst.,* 1999, **32**, 837−838.

[33]   M. Alleaume, F. Leroy, M. Gadret and M. Goursolle, *Acta Crystallogr. Sect.
         B: struct. Sci.,* 1973, **29**, 1994−2000.

[34]   J. J. McKinnon, M. A. Spackman and A. S. Mitchell. *Acta Crystallogr. Sect.
         B: struct. Sci.,* 2004, **60,** 627−668.

[35]   S. K. Wolff, D. J. Grimwood, J. J. McKinnon, D. Jayatilaka and M. A.
         Spackman. 2007, Crystal Explorer 3.0, University of Western Australia, Perth.

[36]   R. F. W. Bader, Y. Tal, S. G. Anderson and T. T. Nguyen-Dang, *Isr. J.
         Chem*., 1980, **19**, 8−29.

[37]   R. F. W. Bader, R. F. W. *Atoms in Molecules: A Quantum Theory*, Oxford,
         Clarendon Press, NewYork, 1995.

[38]   P. Munshi and T. N. Guru Row,   *Acta Crystallogr. Sect. B: struct. Sci.,*
         2006, **62**, 118−127.

[39]   V. Tsirelson, A. I. Stash, V. A. Potemkin, A. A. Rykounov, A. D. Shutalev,
         E. A. Zhurova, V. V. Zhurov, A. A. Pinkerton, G. V. Gurskaya and V. E.
         Zavodnik, *Acta Crystallogr. Sect. B: struct. Sci.,* 2002, **62**, 676−688.

[40]   P. Munshi and T. N. Guru Row, *Acta Crystallogr. Sect. B: struct. Sci.,* 2006,
         62, 612−626.

[41]   A. Volkov, Y. Abramov, P. Coppens and C. Gatti, *Acta Crystallogr.* 2001,
         57, 395−405.

[42]   H. Birkedel, Madsen, D.; Mathiesen, R. H.; Knudsen, K.; Weber, H. P.;
         Pattison and D. Schwarzenbach, *Acta Crystallogr. Sect. A: Found.
         Crystallogr.,* 2004, **60**, 371−381.

[43]   P. Munshi and T. N. Guru Row, *Acta Crystallogr. Sect. B: struct. Sci.,* 2002,
       58, 1011–1017.
[44]   P. Munshi and T. N. Guru Row, *J. Phys. Chem.A,* 2005, **109**, 659–672.
[45]   P. Luger, T. Koritsanszky and M. Weber, *J. Org. Chem.,* 1999, **64**, 1180-
       1190.
[46]   T. S. Koritsanszky and P. Coppens, *Chem. Rev.*, 2001, **101**, 1583–1628.
[47]   A. I. Stash and V. G. Tsirelson, *Crystallogr. Rep*., 2005, **50**, 177–184.
[48]   A. I. Stash and V. G. Tsirelson, *J. Appl. Crystallogr*., 2002, **35**, 371–373.
[49]   D. Stalke, *Che. Eur. J.,* 2011, **17**, 9264–9278.
[50]   P. Politzer and J. S. Murray, *Theor. Chem. Acc.,* 2002, **108**, 134–142.
[51]   V. G. Tsirelson, *Acta Crystallogr. Sect. B: struct. Sci.,* 2002, **58**, 632–639.
[52]   Y. A. Abramov, *Acta Crystallogr. Sect. A: Found. Crystallogr.,* 1997, **53**,
       264–272.
[53]   D. A. Kirzhnits, *Sov. Phys. JETP.*, 1957, **5**, 64.
[54]   E. Espinosa and E. J. Molins, *Chem. Phys.,* 2000, **113**, 5686–5694.
[55]   U. Koch and P. L. A. Popelier, *J. Phys. Chem.,* 1995, **99**, 9747–9754.
[56]   P. Popelier, Atoms in molecules. An Introduction; Prentice Hall: Harlow, U.
       K., 2000; pp 150–153.
[57]   C. Gatti, *Z. Kristallogr.,* 2005, **220**, 399–457.

Charge Density Distribution and Electrostatic Interactions of Ethionamide: An Inhibitor of enoyl acyl carrier protein reductase (InhA) enzyme of *Mycobacterium tuberculosis*

G. Rajalakshmi,[a] Mysore S. Pavan,[b] and P. Kumaradhas [*a,]

[a]Laboratory of Biocrystallography and Computational Molecular Biology
Department of Physics, Periyar University, Salem-636 011, India

[b]Solid State and Structural Chemistry Unit, Indian Institute of Science,
Bangalore 560 012, India

[*]Author to whom correspondence should be addressed: P. Kumaradhas
Corresponding author. Tel.: +91-(0)427-2345520, Fax: +91-(0)427-2345565.
E-mail address: kumaradhas@yahoo.com (P. Kumaradhas)

The experimental and theoretical charge density analysis of ethionamide molecule provides the topological and the electrostatic properties, which allows to understand the nature of intra and intermolecular interactions.